Nucleosynthesis at the proton drip line - a challenge for nuclear physics

H. Schatz*, L. Bildsten†, J. Görres*, T. Rauscher‡, F.-K. Thielemann‡, M. Wiescher*

*University of Notre Dame, Dept. of Physics, Notre Dame, IN 46556, USA
†University of California, Depts. of Physics and of Astronomy, Berkeley, CA 94720, USA
‡Universität Basel, Institut für Physik, CH-4056 Basel, Switzerland

Abstract. The rp-process in X-ray bursts is investigated using a complete and updated nuclear reaction network from H to Sn that is coupled to a one dimensional, one zone X-ray burst model. In particlular we consider 2p-capture reactions that can bridge proton unbound nuclei and therefore accelerate the reaction flow. This allows for the first time the calculation of the actual endpoint of the rp-process. We find that for a 25 s burst the reaction flow reaches already Cd. The consequences for energy production, final composition of the ashes and fuel consumption are discussed. In addition, the influence of the current uncertainties in the nuclear physics data base on the results is investigated and the parameters for which a future experimental determination is most desirable are identified.

I INTRODUCTION

Type I X-ray bursts are thermonuclear flashes on the surface of accreting neutron stars [1–3] (see also the review article [4]). Hydrogen and helium ignite when the accreted layer reaches a critical mass and burn explosively in a thermonuclear runaway. Helium is burned via the 3α-reaction and the αp-process (a sequence of (α,p) and (p,γ) reactions, [5]), which provides seed nuclei for the hydrogen burning via the rp-process [6] (rapid proton capture and β-decays). For a long time the doubly magic nucleus ^{56}Ni was considered to be the endpoint of the rp-process in X-ray bursts, since a captured proton is so weakly bound that photodisintegration can remove it efficiently. In fact most of the previously used reaction networks ended at ^{56}Ni. It was argued, however, that the rp-process might well continue beyond ^{56}Ni and that this would have interesting consequences. Most important is the long standing problem of occasionally observed extremely short burst intervals of the order of several minutes. These burst intervals are too short to accrete enough fuel to power the second burst and can therefore not be explained by the simple thermonuclear flash model. Several solutions to this problem were offered assuming that the second burst is powered by fuel left over from the first burst [5,7]. [8] speculated however, that taking into account processing beyond ^{56}Ni would consume all hydrogen in a single burst and presented therefore an alternative explanation based on mixing of unburned fuel from outer layers into the burning zone. The rp-process beyond ^{56}Ni would also dramatically change the composition of the ashes of the nuclear burning and thus the composition of the outer crust of the neutron star, which would affect neutron star seismology calculations.

The development of nuclear reaction networks beyond ^{56}Ni was hampered in the past by the lack of experimental and theoretical information about the very unstable nuclei at the proton drip line. Nevertheless a few exploratory studies were performed by several authors that either ended at Se [9] or Y [6], or used only 16 nuclei between H and Cd [10]. Given the different results of these studies and the lack of detailed nucleosynthesis calculations beyond Y it seemed to be necessary to investigate the rp-process between Ni and Sn with an updated and complete reaction network.

II NETWORK CALCULATIONS

In a first step, Van Wormer et al. 1994 [11] calculated the rp-process nucleosynthesis between H and Kr for constant temperatures and densities. For the study presented here, we extended their reaction network up to ^{100}Sn (see [12] and references therein).

The most important input parameters for the reaction network are the charged particle reaction rates (proton capture and (p,α)-reactions), the β-decay half-lives and the nuclear masses. The latter are crucial since they determine the particle separation energies and therefore photodisintegration and particle decay rates. Above Ge, the rp-process path enters a region, where for most nuclei along the reaction path none of these parameters are known experimentally and the calculations are therefore based on theoretical models. The parameters used in this study are described in detail in [12]. The charged particle reaction rates were calculated using the Hauser-Feshbach code SMOKER [13]. Uncertainties of less than a factor of two are typical for this method. β-decay half-lives were based on a QRPA code [14]. Comparison of the predicted half-lives (below 100 s) with experimental data for the proton rich nuclei between Ge and Sn yields an average error of a factor of 5.5. For some nuclei above $A = 84$ the half-live can be calculated using the shell model code OXBASH [15], which leads to an improved uncertainty of a factor of 2.7. The nuclear masses were taken from the FRDM (1992) mass model [16]. Comparison with experimental data shows a theoretical error of about 500 keV, which is calculated by decoupling the experimental errors [16]. However, it has also to be taken into account how the uncertainties behave when the mass

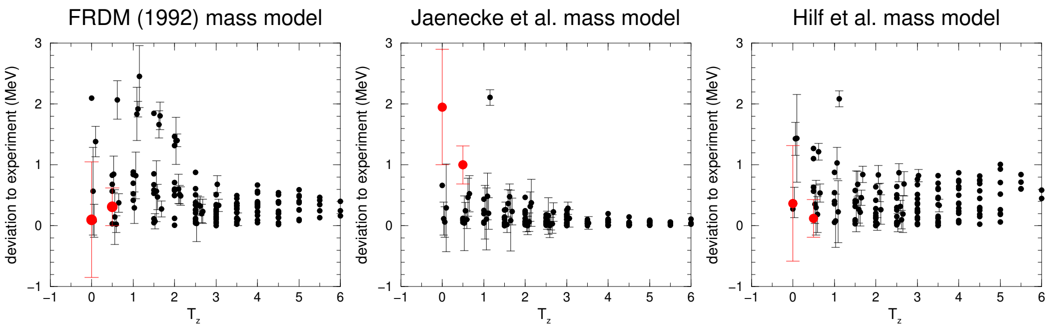

FIGURE 1. The difference of the mass model predictions to experimental nuclear masses as a function of T_z for the proton rich nuclei between Ge and Sn. The errorbars represent the experimental errors. Shown are the results for the FRDM (1992), the Jänecke et al., and the Hilf et al. mass models.

model is extrapolated towards proton rich nuclei. Fig. 1 shows the differences between mass model predictions and experimental data as a function of the z-component of the isospin $T_z = (N - Z)/2$. For comparison we also show the data for the Jänecke et al. mass model [17] and for the older Hilf et al. mass model [18]. For the FRDM (1992) mass model and for the Jaenecke et al. mass model there is a systematic increase in the deviations towards the proton drip line (around $T_z = 0$), even if the larger experimental errors are taken into account. A measure for this is the relation between the theoretical error of all proton rich nuclei in this region (σ) to the theoretical error of the most proton rich nuclei with $T_z \leq 1$ (σ_1). For the FRDM (1992) mass model σ_1 is 70% higher than σ (888 keV instead of 514 keV), while for the Jaenecke et al. mass model σ_1 is more than a factor of 3 larger than σ (286 keV instead of 89 keV). Remarkably, the only mass model that shows no increase in the uncertainty towards more proton rich nuclei but rather a slight decrease is the older Hilf et al. mass model (σ = 466 keV, σ_1 = 412 keV). For the present study the FRDM (1992) mass model was chosen, since it is based on the same description of nuclear structure as the QRPA code. It therefore allows a consistent calculation of all nuclear physics parameters in the network.

We also included the most recent experimental information on the crucial isotopes ^{65}As, ^{69}Br, and ^{73}Rb (see section III A). In addition we considered for the first time 2p-capture reactions [12] that bridge proton unbound nuclei by proton capture on an equilibrium abundance of the unbound nucleus similar to the 3α-reaction. These reactions are typically slow, but they can well compete with the slow β-decays of ^{68}Se and ^{72}Kr thus accelerating the rp-process considerably.

The reaction network was coupled to a 1 dimensional, 1 zone X-ray burst model that calculates temperature and density in the burning zone assuming constant pressure [19]. The raise of the burst is calculated selfconsistently from the generated nuclear energy, while during the burst decline the temperature curve is matched to typical observed luminosity profiles. For the present work a burst with an e-fold luminosity decline timescale of 25 s was chosen. The temperature curve is shown in Fig. 2. The density is initially around 10^6 g/cm^3 and drops down to $2.5{\cdot}10^5$ g/cm^3 when the peak temperature of 2 GK is reached. In all calculations we assumed an initial solar composition.

III RESULTS

A Reaction flow

^{56}Ni was long considered to be the endpoint of the rp-process owing to its long electron capture half-life of $2{\cdot}10^4$ s at X-ray burst conditions and to its low proton capture Q-value that prevents further proton captures at high temperatures because of photodisintegration. This can be seen in Fig. 3 that shows the lifetime of ^{56}Ni against proton capture in the rp-process as a function of temperature and for a typical density of 10^6 g/cm^3. The proton

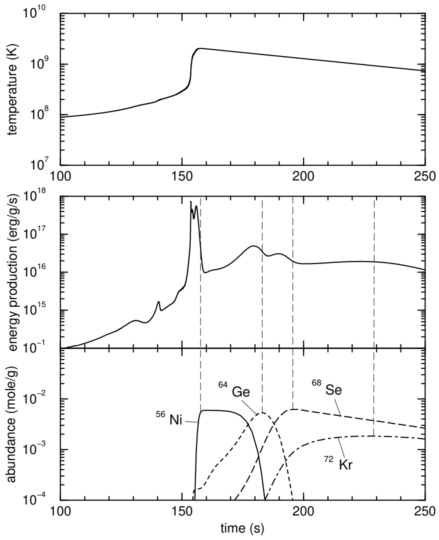

FIGURE 2. The temperature, energy production rate, and the isotopic abundances of the most important waiting points as a function of time.

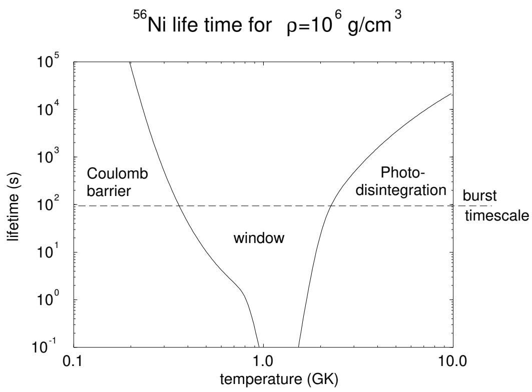

FIGURE 3. The lifetime of ^{56}Ni against proton capture as a function of temperature for a density of 10^6 g/cm^3 and a solar hydrogen abundance. Also indicated is the order of magnitude for the cooling timescale of a typical X-ray burst.

capture lifetime can be estimated quite reliably, since the proton capture Q-values of ^{56}Ni and ^{57}Cu are known experimentally. Proton capture is inhibited at low temperatures due to the Coulomb barrier and at high temperatures due to photodisintegration of ^{57}Cu. However, Fig. 3 also shows that there is a temperature window between 1 and 1.5 GK, where the lifetime of ^{56}Ni is orders of magnitude smaller than the burst timescale. At these conditions ^{56}Ni will be rapidly converted into heavier elements. Fig. 2 shows the abundances of ^{56}Ni and the heavier waiting point isotopes as a function of time. During the temperature raise, the temperature window between 1 and 1.5 GK for processing beyond ^{56}Ni is crossed before the rp-process reaction flow reaches ^{56}Ni. ^{56}Ni is therefore temporarily the endpoint for the rp-process until the temperature window is crossed again during the cooling phase. Then, as Fig. 2 shows, ^{56}Ni is rapidly depleted and the rp-process quickly reaches heavier isotopes.

The next isotopes that were considered as possible endpoints of the rp-process are the rather long lived even Z, $N = Z$ nuclei ^{64}Ge ($T_{1/2} = 64$ s), ^{68}Se ($T_{1/2} = 36$ s) and ^{72}Kr ($T_{1/2} = 17$ s). This has triggered considerable efforts in several laboratories to experimentally investigate the relevant nuclei in this region. However, while the β-decay half-lives are known with good precision, there is still no experimental proton capture Q-value for any of these nuclei. The only information available so far is a β-decay half-life measurement for ^{65}As of 190 ms [20]. In addition upper limits for the lifetimes of ^{69}Br (< 24 ns [21,22]) and ^{73}Rb (< 100 ns [23,24]) can be derived from the nonobservation of these isotopes when certain assumptions for the production cross section in spallation or projectile fragmentation reactions are made. From this it can be concluded that ^{65}As does not proton decay, while ^{69}Br and ^{73}Rb are proton unbound by at least 450 keV and 680 keV respectively. It was therefore speculated that ^{64}Ge can be bridged by fast proton captures and that ^{68}Se delays the rp-process with its full β-decay half-life representing the endpoint of the rp-process. However, the lifetime of ^{68}Se depends sensitively on the proton capture Q-value. This is demonstrated in Fig. 4 that shows the lifetime of ^{68}Se (including β-decay and proton capture) as a function of the proton capture Q-value for a typical temperature of 1.5 GK, a density of 10^6 g/cm^3 and a solar hydrogen abundance. For positive Q-values proton capture reduces the lifetime

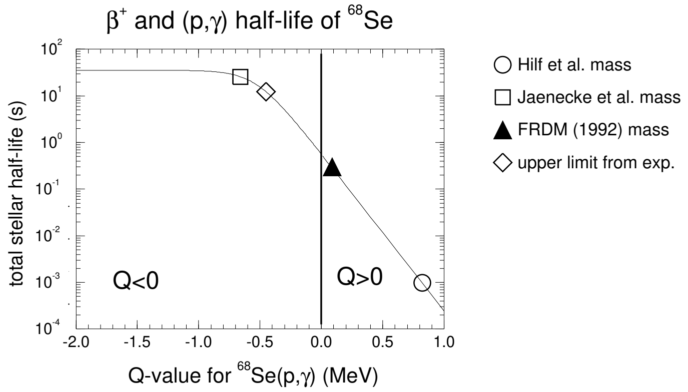

FIGURE 4. The lifetime of ^{68}Se against β-decay and proton capture as a function of the proton capture Q-value for a temperature of 1.5 GK, a density of 10^6 g/cm^3 and solar hydrogen abundance. Indicated are also the predictions of the various mass models as well as the upper limit derived from experimental results.

of ^{68}Se to less than a second and ^{68}Se is not a rp-process waiting point. On the other hand, a negative Q-value does not necessarily imply that β-decay is the only destruction mechanism. There is a range of negative Q-values between 0 and -1 MeV, where the 2p-capture reaction reduces the lifetime of ^{68}Se significantly below its β-decay value. It is therefore not sufficient to determine whether the proton capture Q-value is positive or negative, but its exact value has to be known, as long as it is above -1 MeV. For a lifetime determination of better than a factor of 2 the Q-value has to be known with an accuracy of better than 100 keV. This is about five times better than the accuracy of the FRDM (1992) mass model predictions. An experimental determination of the proton capture Q-value of ^{68}Se would therefore be crucial. The 2p-capture rate on ^{68}Se depends also linearly on the ^{69}Br(p,γ)^{70}Kr reaction rate, but as long as the proton capture Q-value of ^{68}Se is not known experimentally, the respective uncertainties are negleglible. In this study the experimental upper limit for the Q-value of -450 keV was adopted that still leads to a 50% reduction of the ^{68}Se lifetime compared to pure β-decay. For ^{72}Kr similar arguments apply. To summarize, if 2p-capture reactions are taken into account, the lifetimes of the long lived waiting points in the Ge-Kr range are much smaller than previously assumed. It also has to be taken into account that burst timescales of the order of 10 to 100 s are observed and that the 25 s burst discussed in this work has already a cooling timescale of 100 s ($L \propto T^4$, with the luminosity L and the temperature T).

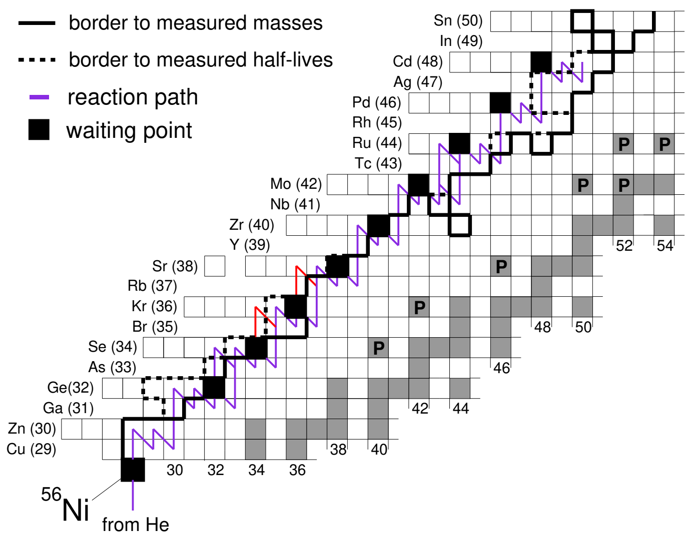

FIGURE 5. The rp-process reaction path above ^{56}Ni. Indicated are the most important waiting points as well as the borders of measuerd masses and half lives.

The complete reaction path above ^{56}Ni is shown in Fig. 5. It can be seen that the rp-process in a 25 s burst proceeds up to ^{98}Cd. The endpoint is reached when the burst timescale equals the summed lifetimes of all waiting points along the reaction path. The dominant waiting points are the even Z, $N = Z$ nuclei between Ge and Cd. Fig. 5 shows that for none of these waiting points experimental proton capture Q-values are available and for the nuclei above ^{76}Sr the β-decay half-lives are not known as well. An experimental determination of these parameters would improve the accuracy of the calculations considerably. Note that the reaction path follows the proton drip line, indicating that neither the Coulomb barrier nor fuel exhaustion are the limiting factors.

B Energy production

Fig. 2 shows the nuclear energy production rate as a function of time during the X-ray burst. A striking feature are the pronounced variations of the energy production rate that span several orders of magnitude. These variations are a consequence of the fact that the energy production drops drastically each time the reaction flow reaches a nucleus with a long lifetime (waiting point). Fig. 2 shows that the first major peak in the energy production is associated with the reaction flow reaching ^{56}Ni, while the next two peaks correlate with the waiting points ^{64}Ge and ^{68}Se. Whether these structures are related to the double burst profiles observed in some X-ray bursts (for example [25]) will have to be investigated using more complex X-ray burst models. It is also interesting to note that 43% of the total burst energy are produced by processing beyond ^{56}Ni during the tail of the burst.

C Final composition

The final composition of the ashes can be found in Fig. 6. Obviously, the endpoint of the rp-process is neither the iron group nor a specific isotope at $A = 64$ or $A = 68$ as it had been suggested before, but a range of nuclei between $A = 68$ and $A = 100$ with a relatively flat distribution. Some material is already accumulated at the end of the network at $A = 100$.

Fig. 7 shows the final overproduction factors in respect to the solar system abundances for the most proton rich isobar in each mass chain, assuming that all unstable nuclei decayed back to stability. β-delayed proton decay was neglected, which was shown to be reasonable for the $A = 96$ and 98 chains by a recent experiment [26]. More experiments of this kind would certainly be important. The distribution of the overproduction factors shows that mainly light p-nuclei are produced with comparable overproduction factors of 10^7-10^8. This is interesting since these nuclei are severely underproduced in standard p-process scenarios. It can be shown [12] that if a small fraction of the burned material (less than 0.03-0.3%) escapes the neutron star, a significant contribution to the galactic nucleosynthesis would be possible. Improved X-ray burst models will have to clarify, whether escape factors of this order of magnitude are reasonable.

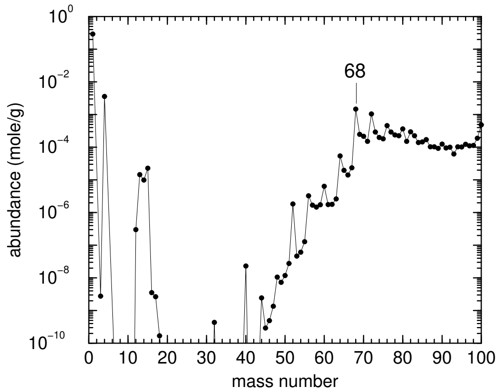

FIGURE 6. The final isotopic abundances summed in each mass chain as a function of mass number.

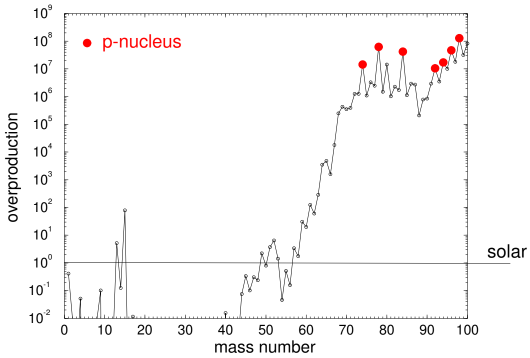

FIGURE 7. The final overproduction factors for the most proton rich isobar in each mass chain as a function of mass number. The overproduction factors are calculated relative to the solar abundances assuming that all unstable nuclei decayed into stable isotopes.

D Fuel consumption

In Fig. 8 we calculated the consumption of hydrogen (^{1}H) and helium (^{4}He) as a function of the luminosity timescale.

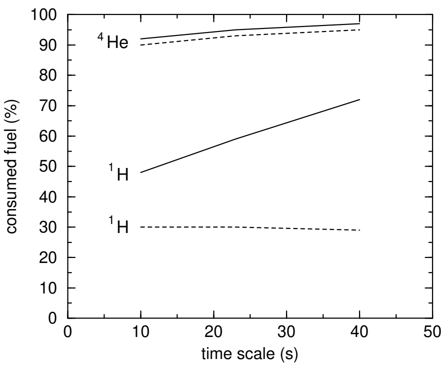

FIGURE 8. The fraction of consumed ^{1}H and ^{4}He fuel as a function of the burst (luminosity) timescale. The dashed lines indicate results from a smaller network ending at ^{56}Ni.

Since the reaction flow reaches the end of the network already for a 25 s burst, the calculations at larger timescales underestimate the fuel comsumption somewhat. Shown are the results for our full reaction network as well as for a network ending at ^{56}Ni. It can be seen that helium is consumed almost completely, independent on burst duration and network size. This is a consequence of the fact that most (70%) of the helium is rapidly burned during the few seconds in the raise of the burst, and that all α-induced reactions occur below ^{56}Ni owing to the Coulomb barrier. On the other hand, Fig. 8 also shows that the use of the full reaction network is essential for calculating the hydrogen consumption. However, even with a full reaction network significant amounts of hydrogen remain unburned (40% for a 25 s burst). This can be understood from the fact that the the transition from the αp-process into the rp-process occurs approximately at ^{41}Sc. Therefore ^{41}Sc is the seed nucleus for the rp-process. Since 10 α-particles (and one proton) are consumed to produce one ^{41}Sc nucleus, and since the ^{1}H/^{4}He number ratio is about 10 (solar value), the proton to seed ration is about 100. From this it follows that in order to consume all hydrogen, the rp-process would have to proceed on average up to $A = 141$. This is not possible, since the here considered cooling timescales of 40-160 s are much shorter than the timescale of the rp-process till $A = 141$ owing to the slow β-decays along the reaction path. Therefore, significant amounts of hydrogen remain unburned and the hydrogen consumption becomes roughly proportional to the burst timescale.

IV CONCLUSIONS

We developed the first complete and updated nuclear reaction network for rp-process calculations beyond ^{56}Ni up to ^{100}Sn. As a first step we used a simple X-ray burst model to investigate the influence of nuclear burning beyond ^{56}Ni. In contrast to [5,6,9] we find that the rp-process in typical X-ray bursts does not end at ^{56}Ni, ^{64}Ge or ^{68}Se, but reaches at least nuclei around $A = 100$. The rp-process beyond ^{56}Ni produces 43% of the burst energy that is released during the burst decline in form of pronounced energy bursts that reflect the properties of the nuclei along the reaction path. We also find that the ashes of the nuclear burning in X-ray bursts, and therefore the outer crust of an accreting neutron star does not consist of iron group nuclei as assumed previously, but of a mostly flat distribution of isotopes between $A = 68$ and $A = 100$. However, in contrast to speculations by [8] the synthesis of these heavier nuclei does not lead to a complete consumption of hydrogen. As a consequence, the models for the explanation of very short burst intervals that rely on the assumption that some hydrogen remains unburned are probably still viable. However, the amount of unburned hydrogen might be lower than assumed. The results obtained depend strongly on theoretical models for the prediction of nuclear masses and β-decay half-lives, that carry large uncertainties. Therefore, an experimental determination of proton capture Q-values and β-decay half-lives of the even Z, $N = Z$ nuclei between Ge and Sn would be most important. In order to constrain waiting point lifetimes better than a factor of two, it is especially important to determine the masses of the waiting point isotopes and the following, eventuelly proton unbound isotones with an accuracy of better than 100 keV - a challenge for theorists and experimentalists.

REFERENCES

1. S. E. Woosley and R. E. Taam, Nature **263**, 101 (1976).
2. L. Maraschi and A. Cavaliere, Highlights of Astronomy **4**, 127 (1977).
3. P. Joss, Nature **270**, 310 (1977).
4. W. H. G. Lewin, J. van Paradijs, and R. E. Taam, Space Sci. Rev. **62**, 233 (1993).
5. S. E. Woosley and T. A. Weaver, in *High Energy Transients in Astrophysics*, Vol. 115 of *AIP Conference Proceedings*, edited by S. E. Woosley (American Institute of Physics, New York, 1984), p. 273.
6. R. K. Wallace and S. E. Woosley, Ap. J. Suppl. **45**, 389 (1981).
7. R. E. Taam, S. E. Woosley, T. A. Weaver, and D. Q. Lamb, Ap. J. **413**, 324 (1993).
8. M. Y. Fujimoto, M. Sztajno, W. H. G. Lewin, and J. van Paradijs, Ap. J. **319**, 902 (1987).
9. T. Hanawa, D. Sugimoto, and M.-A. Hashimoto, Pub. Astr. Soc. Japan **35**, 491 (1983).
10. R. K. Wallace and S. E. Woosley, in *High Energy Transients in Astrophysics*, Vol. 115 of *AIP Conference Proceedings*, edited by S. E. Woosley (American Institute of Physics, New York, 1984), p. 319.
11. L. Van Wormer *et al.*, Ap. J. **432**, 326 (1994).
12. H. Schatz *et al.*, 1997, Phys. Rep., in print.
13. T. Rauscher, F.-K. Thielemann, and K.-L. Kratz, Phys. Rev. C **56**, 1613 (1997).
14. P. Möller, J. R. Nix, and K.-L. Kratz, At. Data Nucl. Data Tab. (1997), submitted.
15. H. Herndl and B. A. Brown, (1997), to be published.
16. P. Möller, J. R. Nix, W. D. Myers, and W. J. Swiatecki, At. Data Nucl. Data Tab. **59**, 185 (1995).
17. J. Jänecke and P. Masson, At. Data Nucl. Data. Tab. **39**, 265 (1988).
18. E. R. Hilf, H. von Groote, and K. Takahashi, in *Proc. 3rd Inter. Conf. Nuclei far from Stability, Cargese* (CERN, Geneva, 1976), Vol. 76-13, p. 142.
19. L. Bildsten, in *The Many Faces of Neutron Stars*, edited by A. Alpar, L. Bucceri, and J. Van Paradijs (Dordrecht, Kluwer, 1997).
20. J. Winger *et al.*, Phys. Lett. B **299**, 214 (1993).
21. B. Blank *et al.*, Phys. Rev. Lett. **74**, 4611 (1995).
22. R. Pfaff *et al.*, Phys. Rev. C **53**, 1753 (1996).
23. M. F. Mohar *et al.*, Phys. Rev. Lett. **66**, 1571 (1991).
24. A. Jokinen *et al.*, Z. Phys. A **355**, 227 (1996).
25. M. Sztajno *et al.*, Ap. J. **299**, 487 (1985).
26. M. Hellström *et al.*, Z. Phys. A **356**, 229 (1996).